Newton-Raphson Based Efficient Model Predictive Control Applied on Active Vibrating Structures

Gergely Takács and Boris Rohal'-Ilkiv

Abstract— **This article presents a computationally efficient model predictive algorithm, applied on an actively controlled vibrating structure. A brief introduction on the experimental device and theoretical background is followed by an analysis of the practical properties, drawbacks and performance of the controller in question. The experimental data presented and interpreted here shows, that the Newton-Raphson based predictive algorithm presents a viable approach to the control of fast sampling systems.**

I. INTRODUCTION

Undesired vibration is present in many engineering applications and fields. It may cause safety, economic or performance related problems. Although passive means of vibration damping are often used as a remedy, in many cases this is not a viable approach. Amongst others, passive vibration damping involves the manipulation of mass and stiffness properties of the system. This can be impractical or prohibitive, especially at low frequencies.

In addition to semi-active methods of vibration control, active vibration attenuation presents itself as a very appealing alternative. Actuators highly integrated to the controlled system exert force on the object. The signal driving the actuators comes from a control system which gains its feedback from sensors also incorporated in the structure.

Simple and obvious choices for control algorithms governing the behavior of the controllers in active vibration attenuation are already extensively used and well investigated. Linear quadratic (LQ) and PID control are a particularly popular choice amongst vibration applications, since do not raise computational speed issues. On the other hand more intricate control schemes offering better performance or guaranteed stability are often neglected, due to the demand on fast sampling.

Functional and safety limits are imposed on all real-life actuators, the ones used in vibration control are no exception. Model predictive control (MPC) is currently the only control scheme offering constraint handling [1]. Use of MPC in active vibration attenuation has been demonstrated in [2], in which the algorithm with the well know quadratic programming on-line formulation has been transcribed directly into machine code to allow maximum computational efficiency. Although the sampling rate demonstrated was quite impressive, this application failed to address the questions of guaranteed stability.

A rather novel approach has been proposed in [3], [4] and consequently in [5] for performing fast, linear predictive control. This theory suggests a computationally effective on-line code, which is capable of constraint handling and guarantees stability, although on the price of sacrificing complete optimality. We shall refer to this method as Newton-Raphson Model Predictive Control (NRMPC) in this work, as the core of the on-line code is essentially reduced to the well-known root searching algorithm.

This article shall introduce a practical implementation of the NRMPC theory on an experimental laboratory device. The possibilities of using NRMPC on a vibration attenuation system with inherent fast dynamics are explored, alongside with evaluating its properties and drawbacks based on simulation and experimental results.

II. LABORATORY SETUP

A laboratory device has been developed to test the the NRMPC algorithm in vibration attenuation applications. This experimental setup consists of an aluminum beam with one end clamped to a support structure, the other left to vibrate freely. This simple model may represent numerous real-life applications of under-damped systems, such as helicopter rotor blades, antennae or solar panels on satellites.

The control objective is to demonstrate vibration damping effects by utilizing Newton-Raphson MPC, by minimizing deflection measured at the beam tip. The role of the control code is to drive the piezoelectric actuators in accordance with the control objective, respecting their physically given constraints and ensuring stability.

A. Experimental Device

Two flat piezoelectric transducers are permanently bonded to opposing sides of the beam's clamped end marked as PZT 1,2 on Figure 1. These two transducers work as actuators, and are electrically connected counter phase. There are additional transducers, short-circuited to prevent electro-mechanical interaction with the structure. The additional transducers can be used either in sensor mode, or to generate a dynamic disturbance force.

Actuator mode piezoelectric transducers are connected to voltage amplifiers, which in turn are driven directly from a

This work was supported by the Slovak Research and Development Agency, and the European Social Fund.

G. Takács and B. Rohal'-Ilkiv are with the Faculty of Mechanical Engineering, Institute of Automation Measurement and Informatics, Slovak Technical University, 812 31 Bratislava, Slovakia Corresponding author: gergely.takacs@stuba.sk

ISBN 978-963-311-369-1

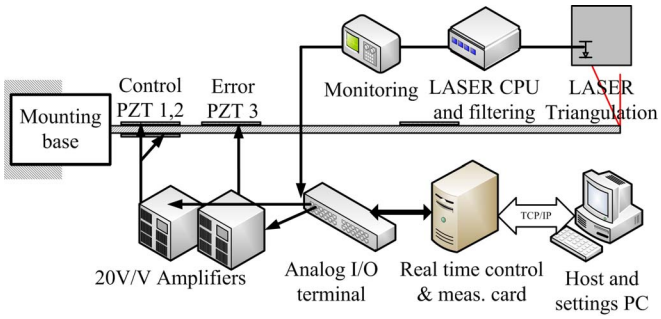

Fig. 1. Experimental device setup scheme.

high sampling rate measuring card. The beam tip deflection is measured by a precision industrial laser triangulation device. Its signal is a direct deviation from the reference equilibrium point, in millimeters. After digital low-pass band filtering, the feedback signal coming from the triangulation sensors is fed to the analog inputs of the same measuring card.

The control code is running on the proprietary real-time operating system using Matlab's xPC Target platform. Its resources are devoted to the control task, the algorithm design has been carried out on an additional designated host machine, connected via Ethernet. The measurement and control chain applied to the vibrating beam is schematically illustrated in Figure 1.

B. Mathematical Identification

To obtain a linear, time invariant state-space mathematical model, an experimental approach was chosen. The actuator mode piezoelectric transducers were driven by a chirp signal, reaching the maximal admissible voltage limits. High voltage levels were required to maximize the force effect of the actuators, in order to minimize signal to noise ratio in-between resonant frequencies. Response at the beam tip has been measured by the triangulation distance sensors.

The raw measurement data was then detrended, filtered. Time series data has been converted using fast Fourier transformation into the frequency domain, where unnecessarily high frequencies were removed by low-pass filtering. This was followed by spectral analysis with frequency-dependent resolution returning, to reduce data set size. The spectral response was then identified by a subspace iteration algorithm [6]. A more detailed description of the experimental hardware, its actual setup and the experimental identification process is given in [7].

III. NRMPC AND ITS IMPLEMENTATION

The formulation introduced in [3] significantly reduces the on-line computational needs of the MPC controller, albeit with the expense of small sub optimality. An extension has been suggested in [4], which reduces the level of this sub optimality to the rather theoretical domain. An enlargement of the initial stabilizable set is achievable trough the optimization of the prediction dynamics described in [5]. The controller, which is physically implemented on the laboratory device, is based on these ideas. After summarizing the theory, an insight is given on the algorithm implementation and the encountered practical problems.

A. Theoretical background

Let us assume, that a system can be modeled by a linear time invariant state-space equation defined by $x_{k+1} = Ax_k + Bu_k$ and $y_k = Cx_k$, with a model order of n_x.

A pre-stabilized loop is created by adding a vector of free variables, the so called perturbation vector $f = [c_k \; c_{k+1} \; \dots \; c_{k+n_c}]^T$ to the control moves. The optimality of the feedback loop may be arbitrarily chosen in the absence of constraints, this implementation for example considered LQ gain. During transients, when the constraints are active, the loop is not optimal and the perturbations will assume nonzero values. Otherwise the perturbations are zero, and a simple LQ control is acting on the system. The control moves and the closed loop system are:

$$u_k = Hx_k + C_c f_k \qquad x_{k+1} = \Phi x_k + Bc_k$$

where Φ is a closed loop matrix $\Phi = (A + BH)$ and H is a fixed feedback matrix optimal in some sense; for example LQ optimal. Vector C_c in the most essential interpretation is responsible for selecting the first element of the development of future perturbations. With optimized prediction dynamics, instead of having a one or an identity matrix in the first position and zeros elsewhere, C_c will be full. The formulation for u implies an augmented system, which is described by the following autonomous state-space equation:

$$z_{k+1} = \Psi z(k) \qquad \Psi = \begin{pmatrix} \Phi & BC_c \\ 0 & A_c \end{pmatrix} \tag{1}$$

where $z = [x \quad f]^T$ is the augmented state vector. Again, A_c contains ones or blocks of identity matrices on the sub-diagonal, and is responsible for shifting the elements in the perturbation vector by a step forward. The development with optimized prediction dynamics assumes this matrix to be full rank, and an unknown in the semi-definite programming (SDP) problem.

The invariance condition is complemented by bounds on the predicted cost, along the trajectories of the autonomous system. As it is indicated later, this bound is necessary for numerical stability. The value of the cost function $\tilde{J} \leq \gamma$ is ensured for all initial conditions of the autonomous system located in the augmented ellipsoidal set, defined by $\varepsilon_z = \left\{ z | z^T P z \leq 1 \right\}$, if the invariance condition for this set is defined by:

$$P - \Psi^T P \Psi > \frac{1}{\gamma} \begin{bmatrix} C^T & H^T \\ 0 & C_c^T \end{bmatrix} D \begin{bmatrix} C & 0 \\ H & C_c \end{bmatrix} \tag{2}$$

where the matrix D is a block matrix containing $D = \mathrm{diag}(I, R)$, containing I as an identity matrix and R as input penalization. Matrix C is the output matrix of the state-space equation, included here as state penalty $Q = C^T C$. Let us assume the presence of the most common process constraint: symmetric limits on the allowable controller output u. Vector $\bar{u}$ shall contain the bounds in the form $|u| \leq \bar{u}$. The feasibility

condition for the augmented ellipsoidal set ε_z is then defined by the following relation:

$$\begin{bmatrix} \bar{u}^2 & \begin{bmatrix} H & C_c \end{bmatrix} \\ * & P \end{bmatrix} \geq 0 \tag{3}$$

where $*$ denotes the symmetric part of the matrix.

If the matrix A_c and vector C_c is also treated as an optimization variable, the size of the stabilizable set can be maximized. Unfortunately this would create a non-convex optimization problem, which can be avoided by performing a nonlinear transformation of variables on the invariance and feasibility conditions [5]. The matrix defining the augmented invariant set ε_z and its inverse may be expressed by the following identities:

$$P = \begin{bmatrix} X^{-1} & X^{-1}U \\ X^{-1}U^T & \bullet \end{bmatrix} \qquad P^{-1} = \begin{bmatrix} Y & V \\ V^T & \bullet \end{bmatrix}$$

$$N = UA_cV^T \qquad M = C_cV^T$$

The blocks of P^{-1} and P which are uniquely determined by X, Y, U, V and by the relation

$$UV^T = X - Y \tag{4}$$

are indicated by the $\bullet$ symbol. By applying the above mentioned cogurence transformation, the conditions for invariance (2) and feasibility (3) will be transformed to:

$$\begin{bmatrix} \gamma I & 0 & D^{1/2}\begin{bmatrix} CY & CX \\ HY+M & HX \end{bmatrix} \\ * & \begin{bmatrix} Y & X \\ X & Y \end{bmatrix} & \begin{bmatrix} \Phi Y + BM & \Phi X \\ N + \Phi Y + BM & \Phi X \end{bmatrix} \\ * & * & \begin{bmatrix} Y & X \\ X & Y \end{bmatrix} \end{bmatrix} \geq 0 \tag{5}$$

$$\begin{bmatrix} \bar{u}^2 & \begin{bmatrix} HY+M & HX \end{bmatrix} \\ * & \begin{bmatrix} Y & X \\ X & Y \end{bmatrix} \end{bmatrix} \geq 0 \tag{6}$$

It is very important to note, that in this formulation the initial stabilizable set is not dependent on the length of the control horizon n_c. It is sufficient to chose the control horizon as a fixed $n_c = n_x$, since the matrix representing the projection of the augmented ellipsoid is independent of the actual horizon length. Finally A_c and C_c may be computed from:

$$A_c = U^{-1}NV^{-T} \qquad C_c = MV^{-1} \tag{7}$$

The initial stabilizable set is defined by matrix Y, as the projection of the augmented ellipsoid ε_z into the x subspace. The part of the x subspace, where the optimal control law is feasible without the need to calculate perturbations is defined by the matrix X, and it is the intersection of the augmented ellipsoid ε_z with the x space. The off-line optimization procedure therefore has to include both these objectives, and is performed based on the following general steps [5]:

Algorithm 1
Off-line NRMPC procedure:

- Ignore constraints and calculate a feedback matrix, which is optimal in some sense.
- Maximize the volume of the projection and intersection of the augmented invariant hyper-ellipsoid to x space, by solving the following SDP:

$$\max\left(-\log\det\begin{bmatrix} Y & 0 \\ 0 & X \end{bmatrix}\right) \tag{8}$$

  subject to conditions defined by (5) and (6), in the optimization variables of X, Y, N and M...
- To determine U and V, factorize X and Y from (4).
- Using relation (7) for N and M solve for A_c and C_c...

By performing this algorithm, a feasible and invariant ellipsoid is created in the augmented space, with the relevant projection and intersection with the x state-space. The appropriate results, are then used as parameters in the on-line NRMPC algorithm, which is described by [4]:

Algorithm 2
On-line NRMPC procedure: At each sampling instant k perform the following minimization:

$$\min_f f_k^T f_k \qquad \text{s.t.} \qquad z_k^T P z_k \leq 1 \tag{9}$$

From this the control signal u is evaluated, and the procedure restarted at the next sampling instant.

It is possible to reformulate the optimization constraint in (9) by partitioning P similarly to that of z as follows:

$$z_k^T P z_k = x_k^T \hat{P}_{11} x_k + 2 f_k^T \hat{P}_{21} x_k + f_k^T \hat{P}_{22} f_k \leq 1 \tag{10}$$

It is convenient to present the transformed optimization constraint (10) as a geometrical problem, and interpret it as the search for the shortest distance of an ellipsoid surface from the origin. If the system origin is already included in the ellipsoid defined by (10), there is no need to perform the optimization, since it is already optimal. Lagrange's method for constrained extrema is used to simplify the optimization above:

$$f = \lambda M \hat{P}_{21} x_k \tag{11}$$

$$\begin{aligned} \Phi(\lambda) &= \hat{P}_{12}[M\hat{P}_{22}^{-1}M - \hat{P}_{22}^{-1}]\hat{P}_{21}x_k + \\ &+ x_k^T \hat{P}_{11} x_k - 1 = 0 \end{aligned} \tag{12}$$

where $M = (I - \lambda\hat{P}_{22})^{-1}$ and λ is the unique real root of $\Phi(\lambda)$. For a given time, there is only one viable solution for λ. This comes from the fact that the gradient can be negative at one tangent point: otherwise the hypersphere representing the optimization variable would contact the hyperellipsoid representing the optimization constraint from the inside. To find the root λ of this equation, Newton-Raphson algorithm can be effectively utilized.

The Newton-Raphson algorithm acts as the single most important operation in the on-line NRMPC procedure, as it is required to find the root of $\Phi(\lambda)$, which in turn is utilized to calculate the perturbation vector. Computational efficiency is evident, as there are no complex matrix operations performed on-line. Computational time grows linearly with the considered system order.

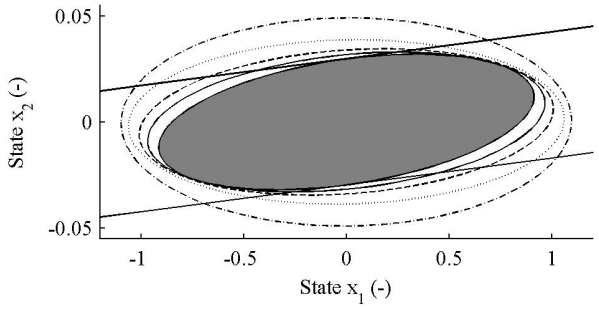

Fig. 2. Projection size with increasing prediction horizon and fixed shift matrix. The innermost ellipse drawn with a solid line denotes $n_c = 2$ steps the dash-dot outer $n_c = 32$ steps ahead prediction.

It is possible to show, that the Newton-Raphson algorithm will converge to a solution quadratically, when initialized with $\lambda = 0$. As practical tests indicated, usually no more than 20 iterations are required to achieve solution with a given precision. Exploiting the eigenvalue-eigenvector properties of $\hat{P}_{22}$ increases computational speed even further.

B. Code implementation

A working version of the NRMPC controller has been developed using Matlab high level scripting language. The off-line routine utilizes the YALMIP interface script [8] to parse linear matrix inequalities (LMI), defined by the invariance and feasibility constraints. This interface directly calls the optimization package SeDuMi [9], for solving the semi-definite program required to evaluate the LMIs. Code testing and simulations have been performed using second order models with various sampling rates.

The on-line code has been also implemented in C language, which allows the use of real-time control under the xPC Target environment, and simulations in Simulink. The C level code utilizes matrix-matrix, matrix-vector and other level 1-3 routines from the basic linear algebra subprograms (BLAS) package [10]. The BLAS library has been compiled to suit the implementation needs [7]. All mathematical operations in the on-line code have been reviewed, unnecessary operations merged or concatenated to allow for maximal computational efficiency. In addition to the NRMPC block, the Simulink scheme also utilizes a product default Kalman observer, blocks for signal routing, input - output drivers and measurement logging facilities.

C. Practical observations on the NRMPC algorithm

While it is possible to use NRMPC according to [3] on highly damped systems, this is certainly not the case with the given active vibration attenuation example, and possibly other under-damped physical systems. The size of the stabilizable set is very small - in fact beyond the point of practical usability. This is clearly illustrated on Fig. 2. The intersection of the augmented ellipsoid with the state space is shown as the shaded area.[1] The volume of the augmented set

[1]Intersection size shrinks with increasing prediction horizon, although in this case with a visually indistinguishable rate - thus not shown on the figure.

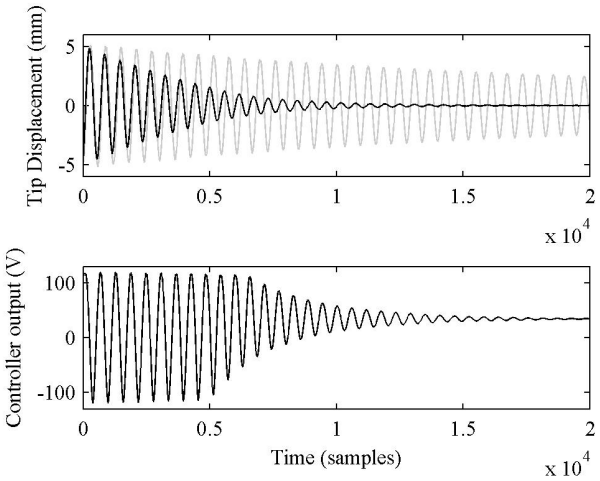

Fig. 3. Uncontrolled (grey) and NRMPC controlled (black) beam tip deflection, caused by an initial deflection of 5mm.

projection - which is incidentally the stabilizable set of initial conditions - is shown as the ellipse outlines with growing volume. The innermost ellipse shows projection assuming 4 steps ahead prediction. Horizon length was then increased by the factor of two, up to the rather unrealistic value of 32 steps shown as the outermost ellipse. Even the very large 32 steps horizon would only allow a maximal initial beam tip deflection of $\pm$0.5mm, which is indeed unreasonably small.

The size of the stabilizable set can be maximized by optimizing prediction dynamics as described in [5]. Here matrices A_c and C_c will be full, the horizon will be fixed and equal to the system order. This approach however may cause numerical problems, when calculating the ellipsoids acting as parameters for the on-line algorithm. This effect has been noted when using under-damped systems, such as the model for the experimental device.

Violation of the invariance condition and constraints has been observed in numerous simulations. In these cases the on-line algorithm parameters contain both extremely large and small numbers, simple matrix multiplications may be erroneous and are prone to numerical problems. A partial remedy to this problem is to set a boundary on the cost function, which directly affects the projection size. There is a cost limit γ, under which the algorithm is reliable, but this way the size of the stabilizable set size is also compromised. Superseding the default tolerance settings and algorithm precision to the obtainable maximum in SeDuMi increased the level of γ by an order of magnitude. This refers to the case of simulations with a second order model of the vibrating beam. We have to note that with other examples, especially higher order models this improvement was not so significant. To preserve invariance and prevent numerical problems, the size of the initial stabilizable set was sacrificed significantly.

IV. EXPERIMENTAL RESULTS

The experimental device described formerly served as a proving ground for the Newton - Raphson predictive control

	f_0 (Hz)	$y_{\max}$ (mm)	ξ (-)
Free:	8.18	12.57	-
NRMPC:	8.86	1.11	11.4
MPMPC	9.3	0.83	15.1

TABLE I
FIRST MODE DAMPING PERFORMANCE

algorithm. All trials utilized a second order model, acting as a base for the predictions calculated by the controller. Since prediction dynamics were also optimized according to [5], horizon length was set equal to the model order. States were penalized by $Q = C^T C$ and inputs by $R = 1E^{-4}$. Input penalization value R has been based on LQ trials; providing a good compromise between performance and controller aggressiveness.

No special steps were taken to increase computational efficiency of the on-line code. An analysis of simulation runtime with respect to components of the on-line code has been performed. This indicated that a significant computational resource is consumed by the product-default Kalman filtering block, and the data logging facilities. Despite of this fact, all the tests were run with a 5kHz sampling rate, some trials were performed going up to a rate of 10kHz. The control run was stable at this level also.

The controller penalization value R and the controller output constraints have been manipulated only to allow for reaching the constraints, so the NRMPC part of the on-line code is active, instead of merely the LQ.

A. Initial deflection

The system response to an initial deflection of 5mm is compared without control, and with the NRMPC controller engaged on Fig. 3. After displacing the beam tip to its starting position, it was left to vibrate freely without any additional disturbance generated. While the controlled response settles to 10% of the original initial displacement in about 1.5 seconds, the uncontrolled response achieves this in more than a magnitude longer time. The controller response indicates, that approximately one second into the experiment the NRMPC portion of the simulation was active, then as the states were entering the invariant intersection of the augmented set, the simple linear quadratic controller took over.

There is a deviation visible in the control signal from the equilibrium value. This is due to the fact that the reference value of the laser triangulation system is arbitrary, and also tends to drift by the fractions of millimeter during the measurement process. To compensate for the static deflection, the controller attempts to constantly supply a mean voltage shifted from zero.

B. Frequency domain

Testing the system response with an initial deflection illustrates the vibration damping capabilities in the time domain. To compare the uncontrolled and NRMPC controlled system response in the frequency domain, the experimental setup was slightly modified. An additional piezoelectric transducer was enabled in the vicinity of the clamped end, not too close to the vibrational nodes as FEM simulations suggest in [11]. This single transducer was engaged in actuator mode, and driven by a chirp signal of the maximal possible voltage amplitude. The upper frequency of the chirp signal passes the second eigenfrequency, but not reaching the third.

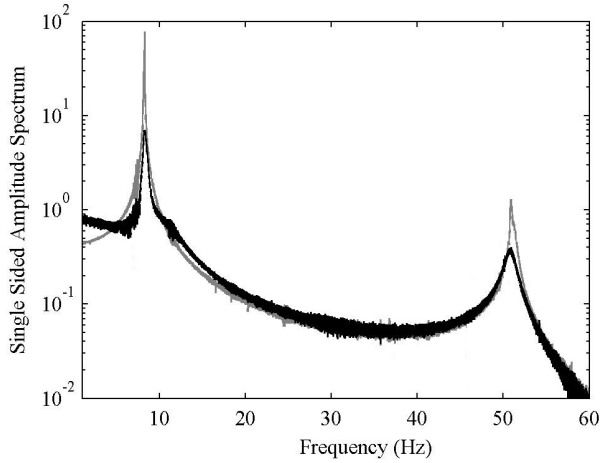

Fig. 4. Uncontrolled (grey) and NRMPC controlled (black) single sided logarithmic amplitude spectrum of the beam tip displacement as a response to a chirp signal.

Fig. 4 shows the logarithmic single sided signal spectra of the beam deflection signal, with respect to the considered bandwidth. The gray line reveals the uncontrolled vibratory response[2], and the black the NRMPC controlled spectrum. Table I lists resonant frequencies f_0, peak deflection values max and damping factor ξ for excitation without and with NRMPC control. Damping performance of multi-parametric programming based MPC is also included for reference.

C. Random Disturbance

Controller performance has been experimentally verified by applying a quasi-random and random disturbance source to the beam. First a medium sized fan has been utilized to create turbulent airflow around the blade, triggering quasi-random mechanical disturbance. Fig. 5 shows beam tip displacement in the time domain, and the corresponding control signal. Maximal controller voltage has been limited to $\pm 50V$ to engage constraints during the control course. Average tip displacement values y_{avg} and peak vibrations $y_{\max}$ are indicated in Table II. Values indicate an excess of 5 fold decrease of average vibrations and 3 fold decrease in peak values when using NRMPC control.

A modal shaker supplied by a random signal has been also used to generate disturbance on the beam. The results of this trial are summarized in Table III, where peak displacement $y_{\max}$ and the decrease factor is indicated. Average vibration displacements y_{avg} with standard deviation σ_y is also shown.

[2]On-line data storage limitations prohibit the use of a slow rate chirp signal, which could cause double the tip deflections indicated here. Magnitude damping ratio enlarges accordingly.

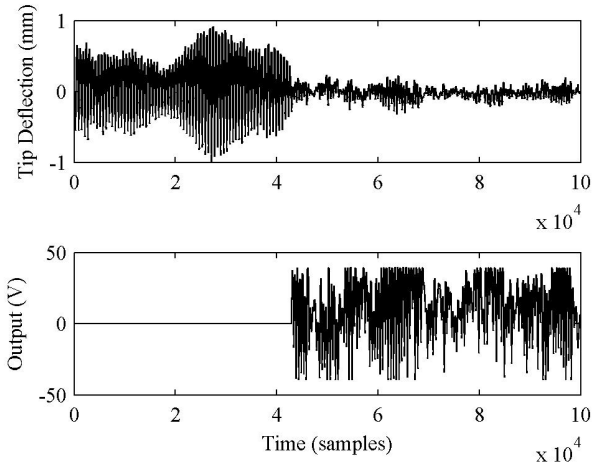

Fig. 5. Uncontrolled and NRMPC controlled beam tip vibration with controller response to a quasi-random excitation.

$y_{\max}$ (mm)	y_{avg} (mm)	
Free:	0.37	1.0
NRMPC:	0.07	0.3

TABLE II
EXCITATION BY FAN

Control signal respects constraints, approaches but never exceeds them. The actual damping performance is better, if the full voltage range of $\pm$120V is engaged on the actuators. Direct physical connection between modal shaker and beam limits the potential effect of actuators, resulting worse performance than in the case of excitation via the fan.

	$y_{\max}$ (mm)	Peak factor (-)	y_{avg} (mm)	σ_y (mm)
Free:	3.64	-	-0.21	$\pm$1.20
NRMPC:	1.53	2.3	-0.23	$\pm$0.49

TABLE III
EXCITATION BY MODAL SHAKER

V. CONCLUSIONS AND FUTURE WORKS

A. Conclusions

A practical implementation of the computationally effective Newton-Raphson model predictive algorithm on an active structure has been presented here. The reliably achieved 10kHz sampling rates indicate a great potential for this approach in the demanding field of active vibration attenuation.

Despite the small theoretical sub optimality, the controller performed well in the laboratory trials, while respecting the process constraints and preserving guaranteed stability. According to the experimental results, the active structure shows significantly increased damping effects, when controlled by NRMPC. Increased damping was evident not only in tests involving an initial deflection, but also under a pseudo-random excitation and in the frequency domain.

In applications a where high sampling rate and large model orders are essential, NRMPC can be an attractive alternative to the simpler control methods, but also offering constraint handling and stability. The NRMPC approach has a potential to outperform multi-parametric MPC (MPMPC) when using higher model orders, although this needs further investigation of the problem.

B. Future Works

In order to increase control bandwidth, higher order models shall be utilized in future works. This would present a possibility to evaluate control performance with more time-consuming on-line operations, involving more complex matrices. The computational speed achieved in these trials suggests, that the sampling rate may be increased, however the inherent sub-optimality of the approach may cause further problems.

VI. ACKNOWLEDGMENTS

The authors gratefully acknowledge the financial support granted by the Slovak Research and Development Agency under the contracts APVV-0280-06 and APVV-0160-07, the ESF project JPD 3 2005/NP1-047 ”PhD students for Modern Industrial Automation in SR”, and reviewers’ comments.

REFERENCES

[1] J. A. Rossiter. *Model-based Predictive Control: A Practical Approach*. First edition. Taylor and Francis (CRC Press). 2003.

[2] A. G. Wills, D. Bates, A. J. Fleming, B. Ninness and S. O. R. Moheimani. Model Predictive Control Applied to Constraint Handling in Active Noise and Vibration Control. *IEEE Transactions on Control Systems Technology*, 16(1): 3-12, January, 2008.

[3] B.Kouvaritakis, J.A.Rossiter, and J.Schuurmans. Effcient Robust Predictive Control. *IEEE Transactions on Automatic Control*, 45(8): 1545–1549, August 2000.

[4] B. Kouvaritakis, M. Cannon, and J.A. Rossiter. Who needs QP for linear MPC anyway? *Automatica*, 38: 879-884, 2002.

[5] M. Cannon and B. Kouvaritakis. Optimizing Prediction Dynamics for Robust MPC. *IEEE Transactions on Automatic Control*, 50 (11): 1892-1597, November 2005.

[6] L. Ljung. *System Identification: Theory for the User*. Second edition. PTR Prentice Hall, Upper Saddle River, NJ. 1999.

[7] G. Takács and B. Rohal’-Ilkiv. Newton-Raphson MPC Controlled Active Vibration Attenuation. In *Proceedings of the 28. IASTED International Conference on Modeling, Identification and Control* Innsbruck, Austria. April 2009.

[8] J. L ofberg. YALMIP : A Toolbox for Modeling and Optimization in MATLAB. *In Proceedings of the CACSD Conference* Taipei, Taiwan. 2004.

[9] J. F. Sturm. Using SeDuMi 1.02, a MATLAB toolbox for optimization over symmetric cones. *Optimization Methods and Software - Special issue on Interior Point Methods* 11-12: 625-653, 1999.

[10] J. Dongarra. Basic Linear Algebra Subprograms Technical Forum Standard. *International Journal of High Performance Applications and Supercomputing* 16 (1):1–111, 2002.

[11] G. Takács. Efficient Model Predictive Control Applied on Active Vibration Control. *PhD Thesis.* Slovak Technical University. Bratislava, Slovakia. May 2009.